Mean velocity and temperature profiles in a sheared diabatic turbulent boundary layer

Dan Li, Gabriel G. Katul, and Elie Bou-Zeid

Citation: Phys. Fluids **24**, 105105 (2012); doi: 10.1063/1.4757660
View online: http://dx.doi.org/10.1063/1.4757660
View Table of Contents: http://pof.aip.org/resource/1/PHFLE6/v24/i10
Published by the American Institute of Physics.

Mean velocity and temperature profiles in a sheared diabatic turbulent boundary layer

Dan Li,[1,a)] Gabriel G. Katul,[2] and Elie Bou-Zeid[1]
[1]*Department of Civil and Environmental Engineering, Princeton University, Princeton, New Jersey 08544, USA*
[2]*Nicholas School of the Environment, Box 80328, Duke University, Durham, North Carolina 27708, USA and Department of Civil and Environmental Engineering, Duke University, Durham, North Carolina 27708, USA*

(Received 18 March 2012; accepted 7 September 2012; published online 16 October 2012)

In the atmospheric surface layer, modifications to the logarithmic mean velocity and air temperature profiles induced by thermal stratification or convection are accounted for via stability correction functions ϕ_m and ϕ_h, respectively, that vary with the stability parameter ς. These two stability correction functions are presumed to be universal in shape and independent of the surface characteristics. To date, there is no phenomenological theory that explains all the scaling laws in ϕ_h with ς, how ϕ_h relates to ϕ_m, and why $\phi_h \leq \phi_m$ is consistently reported. To develop such a theory, the recently proposed links between the mean velocity profile and the Kolmogorov spectrum of turbulence, which were previously modified to account for the effects of buoyancy, are generalized here to include the mean air temperature profile. The resulting theory explains the observed scaling laws in ϕ_m and ϕ_h reported in many field and numerical experiments, predicts their behaviors across a wide range of atmospheric stability conditions, and elucidates why heat is transported more efficiently than momentum in certain stability regimes. In particular, it is shown that the enhancement in heat transport under unstable conditions is linked to a "scale-resonance" between turnover eddies and excursions in the instantaneous air temperature profiles. Excluding this scale-resonance results in the conventional Reynolds analogy with $\phi_m = \phi_h$ across all stability conditions. [http://dx.doi.org/10.1063/1.4757660]

I. INTRODUCTION

The mean velocity and air temperature profiles in sheared diabatic boundary layers are affected by both shear and buoyant forces. In the atmospheric surface layer (ASL), for example, the effects of buoyancy resulting from surface cooling or heating can be more significant than shear in determining the dynamics of the turbulent kinetic energy (TKE). According to Monin-Obukhov Similarity Theory (MOST),[1–3] buoyancy distorts the logarithmic shape of the mean velocity and air temperature profiles via "universal" stability correction functions ϕ_m and ϕ_h, defined for the ASL as[3]

$$\frac{d\bar{u}}{dz}\frac{\kappa_v z}{u_*} = \phi_m(\varsigma), \tag{1}$$

$$\frac{d\overline{T}}{dz}\frac{\kappa_v z}{T_*} = \phi_h(\varsigma), \tag{2}$$

where u is the longitudinal velocity, T is the air temperature, $u_* = \sqrt{\tau_o/\rho}$ is the friction velocity, τ_o is the surface shear stress, ρ is the mean air density, $T_* = -\overline{w'T'}/u_*$ is the surface temperature scale,

a)Author to whom correspondence should be addressed. Electronic mail: danl@princeton.edu. Telephone: 609-933-4802.

$\overline{w'T'} = H_s/\rho C_p$ is the kinematic sensible heat flux density, w is the vertical velocity, κ_v (= 0.40) is the von Karman constant, z is the height above the ground surface, $\varsigma = z/L$ is the atmospheric stability parameter, L is the Obukhov length $L = -u_*^3/\left(\kappa_v \frac{g}{T}\overline{w'T'}\right)$ (neglecting the effect of water vapor on density), g (= 9.81 m s^{-2}) is the gravitational acceleration, and C_p is the specific heat capacity of dry air at constant pressure. The overbar indicates Reynolds-averaged values and the primes denote turbulent excursions from them. These stability correction functions are widely used in hydrological, ecological, and atmospheric studies because they explicitly show how variations in atmospheric stability modify the relationship between turbulent fluxes and mean gradients. They are also critical in numerical models of the lower atmosphere since they are the basis of multiple turbulence closure schemes that are used in climate and weather simulations.[1,3,4]

For neutral atmospheric stability conditions (i.e., $\varsigma = 0$), setting $\phi_m(0) = 1$ and $\phi_h(0) = 1$ (or any other constant[3]) recovers the canonical logarithmic profile shapes for mean velocity and temperature. It is for this reason that ϕ_m and ϕ_h are labeled as stability correction functions: they modify the logarithmic profiles as atmospheric stability changes due to surface heating or cooling. In "idealized micro-meteorological conditions" that are associated with flows that are stationary and planar-homogeneous, with very high Reynolds number, zero mean vertical velocity and pressure gradients, and no Coriolis effects, these stability corrections are assumed to be "universally" independent of surface properties or other boundary conditions except through their effect on the surface fluxes and thus L. As argued in the original work of Monin and Obukhov,[2] the precise form of ϕ_m and ϕ_h can be inferred from experiments.

Since their seminal 1954 publication, many such experiments have been conducted to determine the shapes of ϕ_m and ϕ_h. The functions inferred from the "weighty" Kansas experiments, commonly referred to as the Businger-Dyer (BD) relations,[5] are the corner-stone of micro-meteorology. Many numerical studies, including higher-order closure modeling[6] and large eddy simulations[7] (away from the wall-modeled region where the ϕ_m and ϕ_h need to be imposed), also agree with the BD formulation for ϕ_m and ϕ_h, at least for the range of ς reported in the original Kansas experiments. Table I summarizes many empirically fitted functions for ϕ_m and ϕ_h reported in the literature, including those of BD,[5] Hogstrom,[8] Wilson,[9] Kader and Yaglom,[10] and Brutsaert.[1] Fig. 1 illustrates how some reported ϕ_m and ϕ_h, as well as the model calculations of Vilà-Guerau de Arellano *et al.*[6] (hereinafter VDZ95), vary with ς. While disagreement among these studies can be noted as to the

TABLE I. Stability correction functions for velocity and temperature.

	ϕ_m	ϕ_h
	Unstable conditions	
Businger-Dyer	$\phi_m(\varsigma) = (1 - 15\varsigma)^{-1/4}$	$\phi_h(\varsigma) = 0.74(1 - 9\varsigma)^{-1/2}$
Hogstrom[a]	$\phi_m(\varsigma) = (1 - 19.3\varsigma)^{-1/4}$	$\phi_h(\varsigma) = (1 - 12\varsigma)^{-1/2}$
Wilson	$\phi_m(\varsigma) = (1 + 3.6\lvert\varsigma\rvert^{2/3})^{-1/2}$	$\phi_h(\varsigma) = (1 + 7.9\lvert\varsigma\rvert^{2/3})^{-1/2}$
Kader and Yaglom[b]	$\phi_m(\varsigma) = \begin{cases} 1.04 & 0 < -\varsigma \le 0.1 \\ 0.50\,(-\varsigma)^{-1/3} & 0.3 \le -\varsigma \le 3 \\ 0.21\,(-\varsigma)^{1/3} & -\varsigma \ge 5 \end{cases}$	$\phi_h(\varsigma) = \begin{cases} 0.96 & 0 < -\varsigma \le 0.1 \\ 0.32\,(-\varsigma)^{-1/3} & 0.3 \le -\varsigma \le 3 \\ 0.27\,(-\varsigma)^{-1/3} & -\varsigma \ge 5 \end{cases}$
Brutsaert	$\phi_m(\varsigma) = \begin{cases} \dfrac{0.33 + 0.41\lvert\varsigma\rvert^{4/3}}{0.33 + \lvert\varsigma\rvert} & 0 < -\varsigma \le 14.5 \\ 1 & -\varsigma > 14.5 \end{cases}$	$\phi_h(\varsigma) = \dfrac{0.33 + 0.057\lvert\varsigma\rvert^{0.78}}{0.33 + \lvert\varsigma\rvert^{0.78}}$
	Stable conditions	
Businger-Dyer	$\phi_m(\varsigma) = 1 + 4.7\varsigma$	$\phi_h(\varsigma) = 0.74 + 4.7\varsigma$
Hogstrom	$\phi_m(\varsigma) = 1 + 4.8\varsigma$	$\phi_h(\varsigma) = 1 + 7.8\varsigma$
Brutsaert	$\phi_m(\varsigma) = \begin{cases} 1 + 5\varsigma & 0 < \varsigma \le 1 \\ 6 & \varsigma > 1 \end{cases}$	$\phi_h(\varsigma) = \begin{cases} 1 + 5\varsigma & 0 < \varsigma \le 1 \\ 6 & \varsigma > 1 \end{cases}$

[a]See a review of different stability corrections in Tables VI and VII in Hogstrom.[8]

[b]In Kader and Yaglom,[10] the von-Karman constant was not included in the definitions of L, ϕ_m, and ϕ_h. Here, the von-Karman constant $\kappa_v = 0.40$ is added and thus the coefficients reported here differ from those listed in their original work.

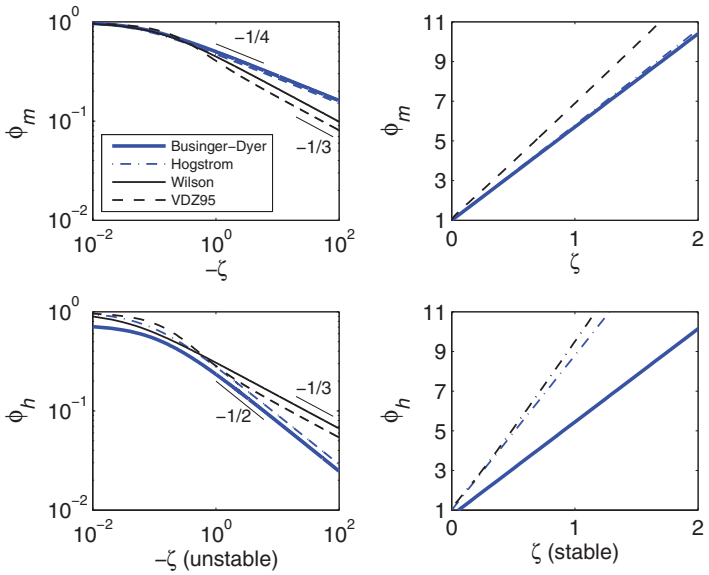

FIG. 1. Stability correction functions for the mean velocity and air temperature under unstable and stable conditions. Under unstable conditions, log-log scales are used to emphasize scaling laws; while under stable conditions, linear axes are used. The functions are as listed in Table I.

exact values of the coefficients in the functions under a given stability regime, it is evident from Fig. 1 that all studies agree that $\phi_m \neq \phi_h$ when $\varsigma < 0$. Under neutral and stable conditions ($\varsigma \geq 0$), nonetheless, some studies support $\phi_m = \phi_h$ but others do not. Some of the scaling laws appear well documented and consistent across all these studies. For example, ϕ_m and ϕ_h increase linearly with increasing ς under stable conditions in all the functions shown in Fig. 1. Under moderately unstable conditions (roughly when $1 < -\varsigma < 5$), the scaling laws in the BD relations appear to follow $\phi_m \sim (-\varsigma)^{-1/4}$ and $\phi_h \sim (-\varsigma)^{-1/2}$. While the free-convection limit is rarely achieved in ASL studies for the idealized micrometeorological conditions ($\varsigma > >1$), ϕ_m and ϕ_h are expected to scale as $(-\varsigma)^{-1/3}$ due to the fact that the effects of u_* cannot be dynamically significant and only the $(-\varsigma)^{-1/3}$ scaling "cancels out" the u_* dependence when $\varsigma > >1$. Although these scaling laws are well established and have been confirmed by a large number of experiments, model calculations, and large eddy simulations, there is no phenomenological theory to explain their onset. In addition, the causes as to why the scaling laws of ϕ_m and ϕ_h with stability are different for $\varsigma < 0$, but not for $\varsigma > 0$, have resisted complete theoretical treatment to date.

Recently, a phenomenological approach was proposed to link the mean velocity profile to the turbulent energy spectrum.[11] The model was then extended to include the effects of thermal stratification on the mean turbulent kinetic energy dissipation rate ($= \varepsilon$) and the eddy-size anisotropy, and consequently on $\phi_m(\varsigma)$, as discussed in Ref. 12. This approach is expanded here to include both momentum and temperature, with a focus on the onset of dissimilarity between momentum and heat across certain stability regimes. By expanding this approach, it is found that interactions between the velocity of turnover eddy and excursions in the instantaneous air temperature profile cannot be ignored as implicitly assumed for the velocity profile, thereby requiring the introduction of a new length scale characterizing the strength of this interaction. This length scale must be explicitly accounted for to successfully recover the stability correction functions for temperature as well as the dissimilarity between momentum and temperature ($\phi_m \neq \phi_h$) for $\varsigma < 0$.

II. THEORY

The mean longitudinal momentum balance and the mean temperature budget for the "idealized micro-meteorological conditions" previously discussed reduce to[3] $\partial \overline{w'T'}/\partial z = \partial \overline{u'w'}/\partial z = 0$. Upon integration with respect to z, these equations result in turbulent shear stress and heat flux near

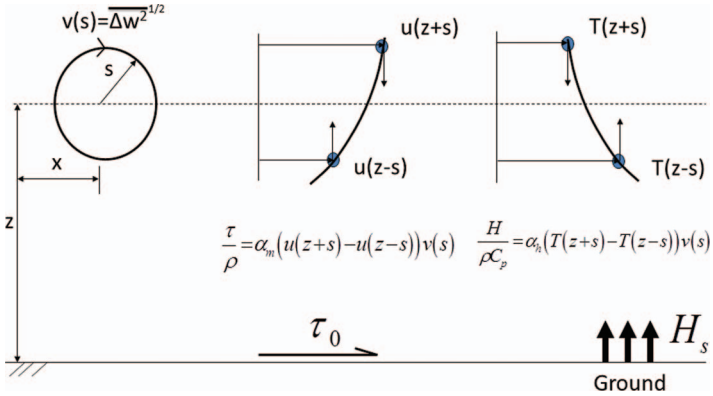

FIG. 2. Turbulent momentum and sensible heat fluxes due to the turnover of an isotropic eddy of radius s acting on a mean velocity and temperature profiles as in Gioia *et al.*[11] and Katul *et al.*[12] The isotropic eddy transfers momentum down at a rate $\rho u\,(z+s)\,v\,(s)$ and up at a rate $\rho u\,(z-s)\,v\,(s)$; similarly, it transfers heat down at a rate $\rho T\,(z+s)\,v\,(s)$ and up at a rate $\rho T\,(z-s)\,v\,(s)$ when the sensible heat flux $H_s > 0$. In Gioia *et al.*,[11] it was argued that the most efficient eddy size that transports momentum to the ground (and hence, by extension, heat from/to the ground) is an eddy of size $s = z$. Katul *et al.*[12] extended the Gioia *et al.*[11] model to thermally stratified conditions. An addition to the Katul *et al.*[12] model is the consideration of the mean temperature profile in this paper.

the ground (but above the buffer layer) identical to their counterparts at an arbitrary height z well above the surface. Extension into the viscous and buffer layers can show that the sum of viscous and turbulent fluxes is constant. Hence $\overline{u'w'}$ and $\overline{w'T'}$ well above the surface are equal to the surface fluxes. These idealized simplifications apply in the so-called log-region of a sheared boundary layer[3] (i.e., the ASL, or the bottom 10%–20% of the atmospheric boundary layer) and imply that L does not vary with z in this region. According to the Gioia *et al.*[11] model illustrated in Fig. 2, the momentum fluxes can be expressed as

$$u_*^2 = \alpha_m v\,(s)\,[\overline{u}\,(z+s) - \overline{u}\,(z-s)] \approx \alpha_m v\,(s)\left[\frac{d\bar{u}\,(z)}{dz} 2s\right]. \tag{3}$$

A straightforward extension to the sensible heat fluxes yields

$$\overline{w'T'} = -\alpha_h v\,(s)\left[\overline{T}\,(z+s) - \overline{T}\,(z-s)\right] \approx -\alpha_h v\,(s)\left[\frac{d\overline{T}\,(z)}{dz} 2s\right], \tag{4}$$

where $v\,(s) = \overline{\Delta w^2}^{1/2}$ is the root mean square of the difference in vertical velocity at the edge and at the center of an isotropic turnover eddy of size s depicted in Fig. 2; $\bar{u}\,(z+s) - \bar{u}\,(z-s)$ is the net kinematic momentum, per unit velocity of the turnover eddy, exchanged between $z+s$ and $z-s$ due to eddies of radius s; similarly, $\overline{T}\,(z+s) - \overline{T}\,(z-s)$ is the net kinematic heat flux, per unit velocity of the turnover eddy, exchanged at height z; and α_m and α_h are proportionality constants.

Similar to Gioia *et al.*,[11] a logical starting point is to assume that eddies that contribute most efficiently to momentum and heat transport are those attached eddies that directly "touch" the surface. Consequently, these "attached-eddies" are of size $s = z$, and Eqs. (3) and (4) reduce to

$$2\frac{\alpha_m}{\kappa_v}\frac{v\,(z)}{u_*}\left[\frac{d\bar{u}\,(z)}{dz}\frac{\kappa_v z}{u_*}\right] = 2\frac{\alpha_m}{\kappa_v}\frac{v\,(z)}{u_*}\,[\phi_m] = 1, \tag{5}$$

$$2\frac{\alpha_h}{\kappa_v}\frac{v\,(z)}{u_*}\left[\frac{d\overline{T}\,(z)}{dz}\frac{k_v z}{T_*}\right] = 2\frac{\alpha_h}{\kappa_v}\frac{v\,(z)}{u_*}\,[\phi_h] = 1. \tag{6}$$

Plausible solutions to Eqs. (5) and (6) must satisfy $\alpha_m\phi_m = \alpha_h\phi_h$. If $\phi_m(0) = \phi_h(0) = 1$ under neutral conditions, α_m must be identical to α_h, which further leads to $\phi_m = \phi_h$ under all stability conditions. A consequence of this finding is that when the phenomenological model in Gioia *et al.*[11] is extended to air temperature with no other modification, it will result in complete similarity between

momentum and heat transport, i.e., the Reynolds analogy. As earlier noted in Table I, there is some evidence supporting the Reynolds analogy under near-neutral and stable conditions; however, the fact that this phenomenological model does not produce the observed dissimilarity between ϕ_m and ϕ_h under unstable conditions[13,14] motivates new refinements. In addition, this shortcoming of the model extension cannot be overcome by simply allowing $\phi_m(0) \neq \phi_h(0)$ as in some studies listed in Table I since that only results in a constant ratio of the two functions under all values of ς. Thus, dissimilarity between momentum and heat for near-neutral conditions alone cannot alter the scaling laws of ϕ_m and ϕ_h with ς.

The solution to Eq. (5) under thermally stratified conditions is given in Ref. 12 and only the main steps leading to the final results are reviewed for completeness. First, Katul *et al.*[12] estimated $v(z)$ from the Kolmogorov theory for locally homogeneous and isotropic turbulence as $v(z) = [k_\varepsilon \varepsilon z]^{1/3}$, where $k_\varepsilon = 4/5$, and ε is the mean TKE dissipation rate. This theory provides a link between $v(z)$ and $z^{1/3}$, but its implementation requires an estimate of ε. Such an estimate can be obtained from the turbulent kinetic energy budget equation subjected to the same idealizations as the mean longitudinal momentum balance and the mean air temperature budget equation. Moreover, these idealizations are complemented by a further assumption that the sum of the pressure transport and flux transport terms is negligible relative to the other terms (this requirement is partially relaxed later though). Hence,[3]

$$\varepsilon = u_*^2 \frac{\partial \bar{u}}{\partial z} + \frac{g}{T}\frac{H_s}{\rho C_p} + \left(-\frac{\partial \overline{w'e^2}}{\partial z} - \frac{1}{\rho}\frac{\partial \overline{w'p'}}{\partial z}\right) \approx u_*^2 \frac{\partial \bar{u}}{\partial z} + \frac{g}{T}\frac{H_s}{\rho C_p} = \frac{u_*^3}{\kappa_v z}(\phi_m - \varsigma), \tag{7}$$

where $e^2 = 0.5\left(u'^2 + v'^2 + w'^2\right)$ is the instantaneous TKE and p' is the turbulent pressure. Note that under neutral conditions, $\varsigma = 0$, $\phi_m(0) = 1$, thus $v(z) = [k_\varepsilon \varepsilon z]^{1/3} = [k_\varepsilon z u_*^3/\kappa_v z]^{1/3}$ $= [k_\varepsilon/\kappa_v]^{1/3} u_* \approx 1.26 u_*$, which is consistent with Townsend's attached-eddy hypothesis[15] that eddies attached to the wall scale with z and have u_* as their characteristic velocity (see Smits *et al.*[16] for a recent comprehensive discussion). Moreover, this value of $v(z) \approx 1.26 u_*$ is commensurate with the value of $\overline{w'^2}^{1/2}$ for near-neutral conditions,[3] as expected when it is this velocity of the turnover eddy that contributes to vertical momentum and heat exchange rates.

With this expression of ε, substituting $v(z)$ into Eqs. (5) and (6) yields the O'KEYPS equations:[17]

$$\frac{2^3 \alpha_m^3 k_\varepsilon}{\kappa_v^4}[\phi_m(\varsigma)]^4 \left[1 - \frac{\varsigma}{\phi_m(\varsigma)}\right] = 1, \tag{8}$$

$$\frac{2^3 \alpha_h^3 k_\varepsilon}{\kappa_v^4}[\phi_h(\varsigma)]^3 \phi_m(\varsigma) \left[1 - \frac{\varsigma}{\phi_m(\varsigma)}\right] = 1. \tag{9}$$

Upon imposing $\phi_m(0) = \phi_h(0) = 1$ under neutral conditions, these equations result in $2^3 \alpha_m^3 k_\varepsilon/\kappa_v^4 = 1$ and $2^3 \alpha_h^3 k_\varepsilon/\kappa_v^4 = 1$, thus $\alpha_m = \alpha_h = \left(\kappa_v^4/2^3 k_\varepsilon\right)^{1/3} \approx 0.21$. As noted in Katul *et al.*,[12] Eq. (8) recovers the –1/4 power-law for small $-\varsigma$, the –1/3 power-law for large $-\varsigma$, and the proportional increase in ϕ_m with an increasing $\varsigma > 0$. However, Eq. (8) does not produce the correct shapes of ϕ_m, which, according to Katul *et al.*,[12] is attributed to (1) finite contributions from the turbulent flux transport of kinetic energy and pressure transport terms in the TKE budget, and (2) more importantly, the anisotropy of the attached eddy in the longitudinal direction due to thermal stratification that results in some departure from the Kolmogorov scaling. After including these two effects, it was shown in Katul *et al.*[12] that Eq. (8) is changed into

$$[\phi_m]^4 \left[\left(1 - (1+\beta)\frac{\varsigma}{\phi_m}\right)\right] = \frac{1}{f_w(\varsigma)}, \tag{10}$$

where $\beta = \left(-\frac{\partial \overline{w'e^2}}{\partial z} - \frac{1}{\rho}\frac{\partial \overline{w'p'}}{\partial z}\right) / \left(\frac{g}{T}\frac{H_s}{\rho C_p}\right)$ is a measure of the contribution from the two transport terms in parenthesis in Eq. (7), which now results in $\varepsilon = \frac{u_*^3}{\kappa_v z}(\phi_m - (1+\beta)\varsigma)$. The

function $f_w(\varsigma) = \left[v(z)/(k_\varepsilon \varepsilon z)^{1/3}\right]^3$ is an estimate of the effect of thermal stratification on the aspect ratio of the turnover eddy since $v(z) = (k_\varepsilon \varepsilon z f_w(\varsigma))^{1/3}$. With an estimate of $f_w(\varsigma)$ based on how the peak of the vertical velocity spectra changes relative to its near-neutral counterpart and setting β to unity (an upper limit in the Kansas experiment), Eq. (10) successfully recovered the correct shape of ϕ_m. The fact that ϕ_m is sensitive to $f_w(\varsigma)$ but not to β, as reported in Katul *et al.*,[12] implies that thermal stratification primarily modulates momentum transport through a change in the aspect ratio of the turnover eddy.

In summary, the model in Katul *et al.*[12] only modifies $v(z)$ compared to the phenomenological model in Gioia *et al.*[11] Since the resulting equation $\alpha_m \phi_m = \alpha_h \phi_h$ from Eqs. (5) and (6) is independent of $v(z)$, it is clear that a direct extension of the model in Katul *et al.*[12] cannot explain the dissimilarity of ϕ_m and ϕ_h under unstable conditions. As such, in addition to the thermal stratification effect on the TKE budget and the eddy aspect ratio, a new mechanism must become significant in the heat transport under unstable conditions, while being suppressed or reduced under stable conditions, to account for such dissimilarity.

III. THE ROOTS OF THE DISSIMILARITY BETWEEN ϕ_m AND ϕ_h

Section I highlighted differences in the observed scaling laws for ϕ_h compared to ϕ_m under moderately unstable conditions, as well as differences in the magnitude of these two functions under all unstable conditions. Straightforward extension of previous models did not capture these differences. In this section, the physical basis of these differences is identified so that it can be incorporated in a generalized phenomenological model for both ϕ_m and ϕ_h.

Equations (3) and (4) postulate that a turnover eddy is passively acting on the "time-averaged" velocity and air temperature profiles, which are smooth and steady. A generalized phenomenological model would relax this assumption starting with the following hypothesis: across the turnover eddy, the spatial excursions embedded in "instantaneous" velocity and temperature profiles could interact with the turnover velocity thereby creating additional "dispersive fluxes" (Fig. 3). Thus, Eqs. (3) and (4) are first reformulated as

$$u_*^2 = \alpha_m \langle v \Delta u \rangle = \alpha_m \left(\langle v \rangle \langle \Delta u \rangle + \langle \tilde{v} \Delta \tilde{u} \rangle \right) = \alpha_m \left(\langle v \rangle \left[u(z+s) - u(z-s) \right] + R_{v\Delta u} \sigma_v \sigma_{\Delta u} \right), \tag{11}$$

$$\frac{H}{\rho C_p} = -\alpha_h \langle v \Delta T \rangle = -\alpha_h \left(\langle v \rangle \langle \Delta T \rangle + \langle \tilde{v} \Delta \tilde{T} \rangle \right) = -\alpha_h \left(\langle v \rangle \left[T(z+s) - T(z-s) \right] + R_{v\Delta T} \sigma_v \sigma_{\Delta T} \right), \tag{12}$$

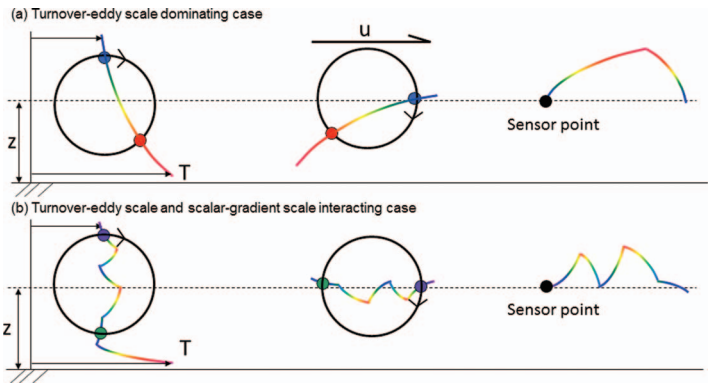

FIG. 3. Turnover-eddy scale dominating case (a) and turnover-eddy scale interacting with fluctuations in the instantaneous temperature-gradient case (b). In (a), the vertical profile of temperature (only temperature is shown here but this argument also holds for velocity) is smooth across the turnover eddy size and the characteristic length scale of temperature is too large to be important; in (b), the vertical profile of temperature is fluctuating so that the characteristic length scale of temperature is reduced and becomes comparable in magnitude to the turnover eddy size. Note that case (b) generates a smaller gradient length scale than case (a).

where Δu and ΔT are variations in the vertical profiles across the turnover eddy (i.e., from $z - s$ to $z + s$); v is the velocity of turnover eddy; brackets denote spatial averaging across the turnover eddy and the tilde indicates excursions from the spatial mean. The $R_{v\Delta u}$ and $R_{v\Delta T}$ are spatial correlation coefficients that account for any interactions between the turnover velocity and excursions in the instantaneous velocity/temperature profiles across the turnover eddy, while σ denotes the standard deviation of a parameter. When the scales modulating v ($= L_v$) and $\Delta u (= L_{\Delta u})$ are sufficiently separated, $R_{v\Delta u} \approx 0$ and the previous phenomenological theory in Eq. (3) is recovered. This scale separation is likely for momentum since the mean velocity varies over length scales commensurate with z, while the velocity of the turnover eddy varies over length scales commensurate to $z^{1/3}$. Hence, even a 50% difference between v and Δu can result in an order of magnitude separation between in L_v and $L_{\Delta u}$. However, when these length scales are comparable, we expect a "boost" in overall fluxes due to interactions (i.e., $R_{v\Delta u}$ and $R_{v\Delta T}$), which were not considered in the original phenomenological model.

This dispersive boost hypothesis is also supported by a complimentary analysis detailed in Appendix A where, starting from momentum and sensible heat flux budgets, it is demonstrated that the sensible heat flux might be significantly increased by the dynamic role of temperature variance σ_T^2 (Eq. (A8)), which can be associated with the excursions in the temperature profiles. As in Eqs. (11) and (12), this boost appears as an "additive term" to the momentum and sensible heat fluxes resulting from the interaction between the turnover eddy and the instantaneous vertical profiles. We point out the striking similarity between Eqs. (11) and (12) and the final equations in Appendix A (e.g., Eqs. (A7) and (A8)) and emphasize that both arguments suggest that there is a missing contribution in the original model. This contribution is associated with excursions in the velocity/temperature profiles across the turnover eddy and their interactions with the turnover eddy.

From a phenomenological perspective, the original models assume that the only length scale controlling the flux-generation process is $s = f_w(\varsigma)\, z$, where $f_w = 1$ in Gioia *et al.*[11] and f_w changes with stability in Katul *et al.*[12] This can only be true when the size of the turnover eddy is much smaller than the characteristic length scale of the velocity or temperature profiles, and thus it solely controls the interactions between the turnover eddy and these profiles (Fig. 3(a)). When buoyancy starts to become important in turbulence generation however, this scale separation is likely to be violated for temperature in certain stability regimes due to possible scale-resonance between the turnover eddy, the mean temperature profile (Fig. 3(b)), and temperature fluctuations (surrogated to a length scale impacting σ_T as shown in Appendix A) embedded within the instantaneous profiles. One possible and measurable indicator of such a scale-resonance effect between the turnover velocity field and the temperature field is the ratio of integral time scales of the turnover velocity and the temperature. The integral time scale of the vertical velocity measures the temporal coherence of the turnover eddy (similar to the scale at which the vertical velocity spectra peak, which was used in Katul *et al.*[12]), while the integral time scale of the temperature fluctuations indicates coherence within the temperature fluctuations. These time scales are often interpreted as horizontal integral length scales when employing Taylor's frozen turbulence hypothesis. While distortions to these integral scale estimates are expected due to the use of Taylor's hypothesis (especially with changes in ς), these distortions are likely to have a weaker impact on the ratio of these length scales, and thus, discussing these ratios is preferred.

Although these horizontal scales are not direct indicators of the characteristic scales of velocity/temperature variations in the vertical direction (i.e., the scales over which $u(z + s) - u(z - s)$ and $T(z + s) - T(z - s)$ vary), spanwise vorticity near the surface (consistent with the turnover eddy model) will act to rotate vertical structures into a horizontal position and induce a correlation between vertical and horizontal integral scales, as shown in Fig. 3. Here, we assume that the ratios of integral scales for w, u, and T in the horizontal direction (as inferred from Taylor's hypothesis), when close to unity,can indicate a scale-resonance potential. In the following part, two data sets collected in the ASL over a lake and a glacier are used to calculate the integral length scales of w, u, and T in the streamwise direction. Details about the two data sets, quality control measures, and calculations of the stability parameter can be found in Vercauteren *et al.*,[18] Bou-Zeid *et al.*,[14,19] and Li *et al.*[20] The integral length scales are calculated by integrating the autocorrelation functions up to their first zero-crossings and invoking Taylor's hypothesis.[3] The lake data set covers unstable to

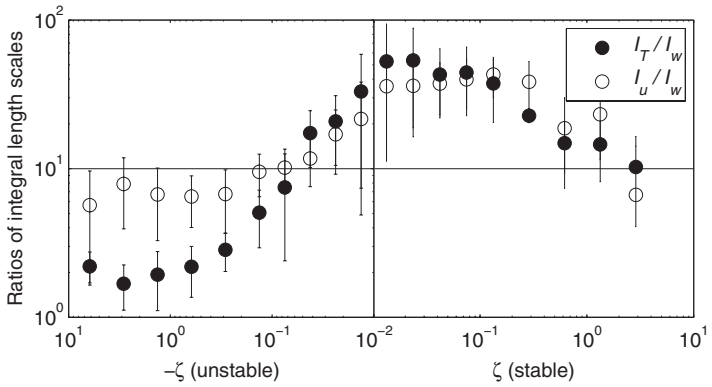

FIG. 4. Ratios of the integral length scale of the steamwise velocity/temperature to that of the turnover velocity.

slightly stable conditions and the glacier data set covers slightly stable to very stable conditions so that the combination of two data sets provides a complete picture of scale-resonance between the turnover eddy and the vertical profiles of mean velocity/temperature over a wide range of stability regimes.[20]

As shown in Fig. 4, the ratio of integral length scales of the longitudinal velocity and the turnover velocity (I_u/I_w) is on the order of 10–100 for all ς so that interactions between the turnover velocity and the velocity gradients across the eddy remain largely controlled by the scale of the turnover velocity. The fact that a large scale-separation exists between the mean velocity and the turnover velocity under all stability conditions implies that thermal stratification affects momentum transport by means of modifying the turnover eddy only, as postulated in Katul *et al.*[12]

Similarly, it is clear that under near-neutral and stable conditions, the ratios of the integral length scales of the temperature and the turnover velocity (I_T/I_w) are much larger than unity. However, as the instability increases, the ratio I_T/I_w decreases to order unity when $-z/L > 0.2$, implying that scale separation is significantly reduced. A possible contributing mechanism to this reduction in scale-separation is the increase in I_w under unstable conditions observed when buoyancy contributes to the generation of eddies.[12,21] But it is the decrease in the integral length scale of temperature when $-z/L > 0.2$ that turns out to be more important in reducing the scale-separation (not directly shown here but can be inferred from Fig. 4). Consequently, the interactions of the turnover eddy with the mean as well as with the instantaneous temperature profile jointly contribute to heat transport. As the atmosphere becomes more unstable, the scale-resonance between the turnover velocity and the temperature fluctuations is enhanced and violates the implicit assumption in the original phenomenological model.

IV. GENERALIZING THE PHENOMENOLOGICAL MODEL

To include the possible effect of scale-resonance between the turnover velocity and temperature excursions and to provide a complete framework for studying stability correction functions for both momentum and temperature, new scales that characterize the variability in these vertical profiles, $f_u(\varsigma)$ and $f_T(\varsigma)$, are hence needed in the model. With $(d\bar{u}(z)/dz)\,2s = (d\bar{u}(z)/dz)\,zf_u(\varsigma)$ and $\left(d\overline{T}(z)/dz\right)2s = \left(d\overline{T}(z)/dz\right)zf_T(\varsigma)$ substituted into Eqs. (3) and (4), we obtain

$$u_*^2 = \alpha_m \left(k_\varepsilon \varepsilon\, z f_w(\varsigma)\right)^{1/3} \left[\frac{d\bar{u}(z)}{dz} z f_u(\varsigma)\right], \tag{13}$$

$$\overline{w'T'} = -\alpha_h \left(k_\varepsilon \varepsilon\, z f_w(\varsigma)\right)^{1/3} \left[\frac{d\overline{T}(z)}{dz} z f_T(\varsigma)\right]. \tag{14}$$

Equations (13) and (14), together with $\varepsilon = \frac{u_*^3}{\kappa_v z}(\phi_m - (1+\beta)\varsigma)$ and the definitions of ϕ_m and ϕ_h, lead to

$$[\phi_m]^4 \left[\left(1 - (1+\beta)\frac{\varsigma}{\phi_m}\right)\right] = \frac{1}{f_w(\varsigma)}\frac{1}{(f_u(\varsigma))^3}, \tag{15}$$

$$[\phi_h]^3 \phi_m \left[\left(1 - (1+\beta)\frac{\varsigma}{\phi_m}\right)\right] = \frac{1}{f_w(\varsigma)}\frac{1}{(f_T(\varsigma))^3}. \tag{16}$$

Another theoretical approach leading to a formulation similar to Eq. (16) is presented in Appendix B based on the Kolmogorov theory[22] for the velocity spectrum and the Kolmogorov-Corrsin theory[22,23] for the temperature fluctuation spectrum. The new derivation presented in Appendix B also argues that the heat flux is generated through interactions between the turnover velocity and "macro-scale" variations in the instantaneous temperature profile ($= \overline{\Delta T'^2(s)}^{1/2}$) when $s = z$, with $\overline{\Delta T'^2(z)}^{1/2}$ being proportional to $\bar{T}(z+s) - \overline{T}(z-s)$. This approach predicts that ϕ_h differs from ϕ_m partly due to differences in integral length scales ($I_T/I_w \neq I_u/I_w$) and intermittency parameters, which are larger for heat than horizontal velocity in the inertial subrange because of "contamination" due to prevalent ramp structures dominating the temperature time series.[24]

To solve Eqs. (15) and (16), expressions for f_w, f_T, and f_u are required. An estimate of $f_w(\varsigma)$ is already given in Katul *et al.*[12] based on an interpolation of the functions presented in Kaimal and Finnigan[21] for the spectral peaks in the vertical velocity derived from the Kansas experiment. The interpolated $f_w(\varsigma)$ is slightly revised in this study compared to the function given in Katul *et al.*[12] to ensure that $\phi_m$scales linearly with ς under all stable conditions, which according to Eq. (15) requires $f_w(\varsigma) \sim \varsigma^{-4}$, yet ensuring the smoothness of the function f_w at $\varsigma = 0$. Comparing Eqs. (15) and (16) to Eqs. (11) and (12), respectively, reveals that f_u and f_T act like "amplification factors" that account for interactions between the turnover eddy and the excursions in the vertical profiles. Due to the scale separation between the turnover velocity and the characteristic length scale for the velocity profile (Fig. 4), we use $f_u(\varsigma) = 1$ under all stability conditions. Through similar reasoning, we use $f_T(\varsigma) = 1$ under neutral and stable conditions; while under unstable conditions, f_T increases gradually in accordance with Fig. 4 to represent the scale-resonance between the turnover eddy and the temperature gradients. In addition, f_T approaches f_w asymptotically as instability increases. This follows from the fact that the ratio of horizontal integral length scales of the vertical velocity and temperature, which is used as an estimate of the ratio of the characteristic length scales of the turnover eddy and the temperature gradients, approaches unity gradually as instability increases, as shown in Fig. 4. The fact that the characteristic length scale of the temperature gradients becomes important gradually (ratio of the integral scale decreases smoothly in Fig. 4) indicates that f_T should increase more slowly than f_w. It also needs to be pointed that the increase in f_T is mainly in the range $-5 < \varsigma < -0.2$; this is related to the significant reduction in the scale-separation in this regime as shown in Fig. 4. It turns out that it is the rapid increase of f_T in this range of ς, compared to f_u that results in different scaling laws for temperature, $(-\varsigma)^{-1/2}$, when compared to momentum, $(-\varsigma)^{-1/4}$. From these theoretical and observational constraints, a function form for f_T can be inferred.

The final expression of f_w, f_T and f_u are as follows (Fig. 5):

$$f_w(\varsigma) = \begin{cases} 1 - \dfrac{0.38}{0.55}\left[1 - \exp(25\varsigma)\right] & \varsigma \le 0 \\ \left(1 + \dfrac{25}{4}\dfrac{0.38}{0.55}\varsigma\right)^{-4} & \varsigma > 0 \end{cases}, \tag{17}$$

$$f_T(\varsigma) = \begin{cases} \left(\dfrac{1 + 10.5\,|\varsigma|^{1.5}}{1 + 0.3\,|\varsigma|^{1.5}}\right)^{1/3} & \varsigma \le 0 \\ 1 & \varsigma > 0 \end{cases}, \tag{18}$$

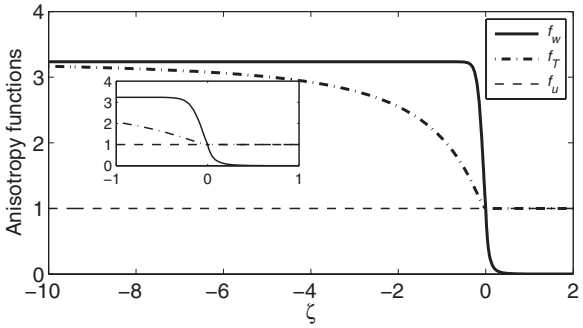

FIG. 5. The anisotropy functions used to recover the stability correction functions. For mean velocity, u, the anisotropy function remains unity due to the large scale-separation between the characteristic length scale of a turnover eddy and the characteristic length scale of the mean velocity field. So does the anisotropy function for temperature under neutral and stable conditions. However, as instability increase, the anisotropy function for temperature increases in accordance with the reduction in the scale separation. Under very unstable conditions, the scale separation is minimal and f_T asymptotically approaches f_w. The inset is a close-up for the range of $-1 \leq \zeta \leq 1$.

$$f_u(\zeta) = 1. \tag{19}$$

Note that f_w is interpolated based on the Kansas experiments and some characteristics are not altered by the interpolation. For example, under very unstable conditions, f_w should approach a constant value of 3.25. Similarly, f_T is inferred based on the scale-resonance between the vertical velocity and the temperature gradients (Fig. 4). Even though this inference does not exactly determine the expression of f_T, it constrains its shape sufficiently so that the inferred expression depicted in Fig. 5 will be an adequate working model for f_T.

V. MODEL EVALUATION

Substituting the expressions of f_w, f_T and f_u into Eqs. (15) and (16) and setting $\beta = 0.5$, the average value deduced from the Kansas experiment yields the stability correction functions ϕ_m and ϕ_h shown in Fig. 6. It is evident that the new functions given by the proposed phenomenological model are well within the range of previously proposed and validated functions. All the widely observed and accepted scaling laws are recovered, such as the linear law under stable condition and the –1/3 power law under very unstable conditions. Particularly, the different scaling laws for momentum (–1/4 power law) and temperature (–1/2 power law) under moderately unstable conditions are also recovered with the contribution from f_T. It should be pointed out that the β value slightly changes the profiles especially when the heat flux is large (i.e., at large $-\zeta$); nonetheless, the range over which the β value varies is quite limited, from 0 to 1, so that the uncertainty in β does not change the results qualitatively.

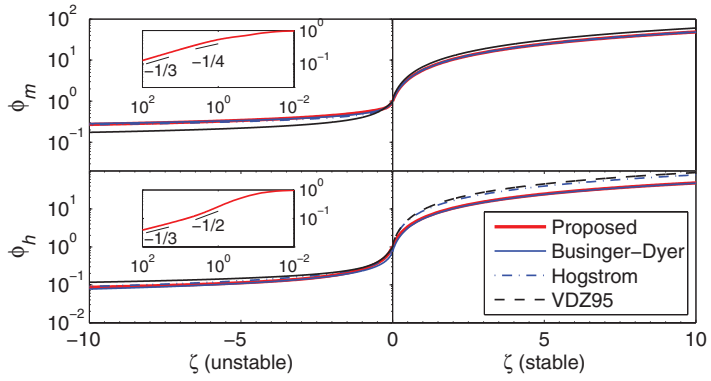

FIG. 6. The stability correction functions for mean velocity ϕ_m and mean temperature ϕ_h.

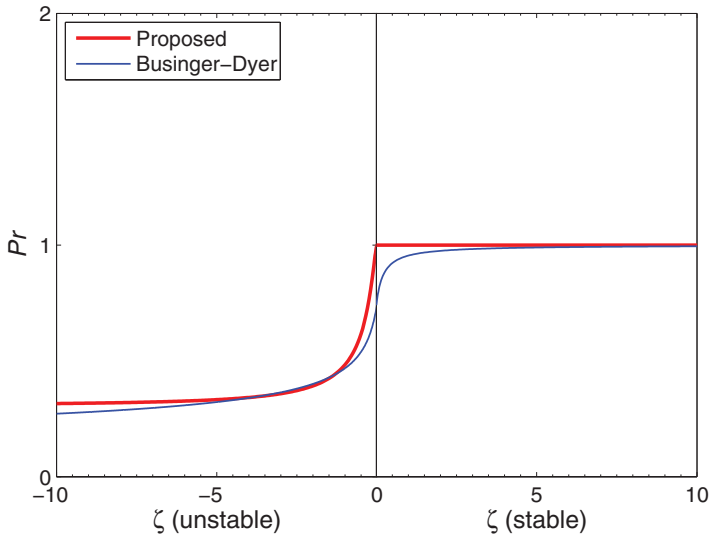

FIG. 7. The turbulent Prandtl number (Pr) calculated from stability correction functions.

The ratios of stability corrections functions for temperature and mean velocity define a turbulent Prandlt number:

$$\mathrm{Pr} = \frac{\phi_h}{\phi_m} = \frac{f_u}{f_T}. \tag{20}$$

As shown in Fig. 7, the deviation of turbulent Prandtl number from unity arises from the difference between f_T and $f_u$under unstable conditions. Thus the decrease in the turbulent Prandlt number as instability increases, or the enhancement of heat transport relative to momentum transport, is attributed to the interactions between the turnover eddy and excursions in the temperature profile within this framework, and is in agreement with the results of Li and Bou-Zeid.[13] Under neutral and stable conditions, the turbulent Prandlt number remains unity simply because of the large scale-separation between the turnover eddy size and the characteristic length scale for the velocity/temperature profiles. In that regime, the transports of momentum and heat are controlled primarily by the size of attached eddies with neither momentum nor heat transport enhanced or diminished, according to the proposed model.

This scale separation is also reduced as stability increases under stable conditions (Fig. 5) but it decreases very similarly for u and T and would thus not affect the ratio of ϕ_m over ϕ_h. For the stability range covered by the data in Fig. 5, this decrease is not sufficient to allow the variability in the gradients to interact with the turnover velocity. Higher stabilities might reduce this scale separation further.

One should also note that the value of the Prandtl number under neutral and stable condition in the proposed model is restricted by the assumption that $\phi_m = \phi_h$ under neutral stability and thus $\alpha_m = \alpha_h$ (see discussion after Eq. (6)). From Table I, one can observe that not all empirical models predict $\phi_m = \phi_h$ and thus $Pr = 1$ under neutral and stable conditions.[25] The proposed model can be modified to yield a different Prandtl number under neutral and stable conditions if evidence supports other values. However, what emerges from the model inherently is the scaling of the stability functions and the fact that their ratio under neutral and stable conditions remains constant.

VI. SUMMARY AND CONCLUSIONS

A new phenomenological model is proposed to explain the scaling laws and the shape of the stability correction functions for mean velocity ϕ_m and temperature ϕ_h in a sheared diabatic turbulent boundary layer. This is the first phenomenological framework that connects the attached eddy hypothesis, the spectral peaks in the turbulent temperature and velocity series, the Kolmogorov

energy cascade for velocity and temperature within the inertial subrange, and the stability correction functions for heat and momentum in the atmosphere. The aim is to provide a theoretical explanation for scaling of ϕ_m and ϕ_h with stability and to explain the dissimilarity between momentum and heat transport under unstable conditions. It is found that a straightforward extension of the original model in Katul *et al.*[12] to temperature results in absolute similarity between ϕ_m and ϕ_h (i.e., Reynolds analogy), given the similarity in the turnover eddy acting on the mean profiles. Hence, such an extension cannot recover the widely reported different scaling laws for ϕ_h (–1/2 power law) when compared to ϕ_m (–1/4 power law) in the unstable regime. The failure of this original model, when extended to temperature, is traced to the interaction between the turnover eddy and excursions in the instantaneous temperature profiles. This interaction results in dispersive fluxes that augment heat flux, but do not affect momentum flux. Starting from the momentum and sensible heat flux budgets, it is further demonstrated that the dynamic role of temperature variances modulates the length scale characterizing the variability in the instantaneous temperature profile and thus enables the scale resonance causing the dispersive fluxes. These findings then provide the basis for a refinement to the original phenomenological model. This refinement is introduced via a new adjustment to the attached eddy size (i.e., resembling an anisotropy ratio) representing the effect of interactions between the turnover eddy and the excursions in the temperature vertical profiles.

Ignoring these adjustments in the momentum transport is justified by the fact that the integral length scale of the longitudinal velocity is at least one order of magnitude larger than the size of the turnover eddy. However, this is demonstrated not to be the case for temperature under unstable conditions. The integral length scale of the temperature profile, which is approximated by the integral length scale of the temperature time-series measured at a given point, becomes comparable to the integral length scale of the turnover velocity. The immediate implications then are that the mean temperature difference at the two end-points of the turnover eddy is no longer a viable indicator of the size of excursions in the temperature profile across the turnover eddy; but rather, a new length scale characterizing the size of these excursions has to be introduced. The scale-resonance or interactions between the turnover eddy and the excursions in the temperature profiles enhance the heat transport and result in dissimilarity between momentum and temperature. It is also this scale-resonance mechanism that is responsible for the decrease in the turbulent Prandtl number under unstable conditions.

With this new length scale incorporated into the phenomenological model, the stability dependence of the generalized model is now guided by the ratio of integral length scales and successfully recovers the –1/2 power law scaling law for ϕ_h, as well as the dissimilarity between momentum and temperature under unstable conditions. Under neutral and stable conditions, ϕ_h remains the same as, or proportional to ϕ_m.

ACKNOWLEDGMENTS

This work is supported by National Science Foundation (NSF) under CBET-1058027 and AGS-1026636. G. G. Katul acknowledges support from NSF through Grant Nos. NSF-EAR-1013339, NSF-AGS-1102227, and NSF-CBET-103347, the United States Department of Agriculture (2011-67003-30222), and the U.S. Department of Energy (DOE) through the office of Biological and Environmental Research (BER) Terrestrial Ecosystem Science (TES) Program (DE-SC0006967). The authors would like to thank Professor Marc Parlange, Dr. Hendrik Huwald, Dr. Chad Higgins, and the rest of the team of the Environmental Fluid Mechanics and Hydrology Laboratory at the Swiss Federal Institute of Technology—Lausanne for the collection of the lake and glacier datasets described here. The authors also thank Professor Jordi Vilà-Guerau de Arellano for providing them the model results in VDZ95.

APPENDIX A: DYNAMIC ROLE OF TEMPERATURE VARIANCES IN INDUCING DISSIMILARITY BETWEEN MOMENTUM AND HEAT TRANSPORT

The momentum and sensible heat flux budgets are considered for the idealized micrometeorological conditions previously assumed. These budgets are intended to illustrate the causes of

dissimilarity between momentum and sensible heat for these idealized conditions. These budgets reduce to[3,26]

$$\frac{\partial \overline{u'w'}}{\partial t} = 0 = -\overbrace{\overline{w'w'}\frac{d\overline{u}}{dz}}^{T_1} - \underbrace{\frac{\partial \overline{w'w'u'}}{\partial z}}_{T_2} - \overbrace{\frac{1}{\bar{\rho}}\left(\overline{u'\frac{\partial p'}{\partial z}} + \overline{w'\frac{\partial p'}{\partial x}}\right)}^{T_3} + \underbrace{\frac{g}{\overline{T}}\overline{u'T'}}_{T_4}, \tag{A1}$$

$$\frac{\partial \overline{w'T'}}{\partial t} = 0 = -\overbrace{\overline{w'w'}\frac{d\overline{T}}{dz}}^{T_1} - \underbrace{\frac{\partial \overline{w'w'T'}}{\partial z}}_{T_2} - \overbrace{\frac{1}{\bar{\rho}}\overline{T'\frac{\partial p'}{\partial z}}}^{T_3} + \underbrace{\frac{g}{\overline{T}}\overline{T'T'}}_{T_4}. \tag{A2}$$

Terms T_1, T_2, T_3, and T_4 are the flux/gradient production, turbulent transport, temperature-pressure interaction (a de-correlation term), and buoyant production, respectively. If a conventional closure model is applied to term T_3,[3,27,28] then

$$\frac{1}{\bar{\rho}}\left(\overline{u'\frac{\partial p'}{\partial z}} + \overline{w'\frac{\partial p'}{\partial x}}\right) = C_1\frac{\overline{u'w'}}{\tau}, \tag{A3}$$

$$\frac{1}{\bar{\rho}}\overline{T'\frac{\partial p'}{\partial z}} = C_2\frac{\overline{w'T'}}{\tau} - \frac{1}{3}\frac{g}{\overline{T}}\overline{T'T'}, \tag{A4}$$

where τ is a relaxation time scale defined by the ratio of the TKE and its mean dissipation rate, and C_1, C_2 are closure constants. This relaxation time scale is a measure of how fast energy-containing eddies dissipate or lose their coherency (or de-correlate in time). Under some conditions, this time scale can also be interpreted as the time scale over which the turbulence comes into a local equilibrium with the surrounding mean velocity gradient.[29] The turbulent flux transport terms can also be conventionally parameterized by a gradient-diffusion closure, the simplest being a model of the form[30]

$$\frac{\partial \overline{w'w'u'}}{\partial z} = K_1\frac{\partial \overline{w'u'}}{\partial z}, \tag{A5}$$

$$\frac{\partial \overline{w'w'T'}}{\partial z} = K_2\frac{\partial \overline{w'T'}}{\partial z}, \tag{A6}$$

where K_1, K_2 are diffusivities. Since the analysis here is restricted to the constant-flux or stress regions ($\partial\overline{w'T'}/\partial z = \partial\overline{w'u'}/\partial z = 0$), the turbulent flux transport terms are thus zero (or small relative to the production terms). With Eqs. (A3)–(A6), the momentum and heat flux budgets can be re-arranged to yield[31]

$$\overline{u'w'} = \frac{\tau}{C_1}\left(-\overline{w'w'}\frac{d\overline{u}}{dz} + \frac{g}{\overline{T}}\overline{u'T'}\right), \tag{A7}$$

$$\overline{w'T'} = \frac{\tau}{C_2}\left(-\overline{w'w'}\frac{d\overline{T}}{dz} + \frac{4}{3}\frac{g}{\overline{T}}\overline{T'T'}\right). \tag{A8}$$

It is evident that the resulting equations are similar to Eqs. (10) and (11) as the first-term on the right-hand side is the conventional term that would have been predicted from the original phenomenological model. The second term on the right-hand side represents the buoyancy effect on momentum and heat transfer, which suggests that the covariance between the longitudinal velocity and temperature plays a role in any gradient-diffusion argument beyond the thermal stratification effects on $\overline{w'w'}$, partly characterizing the turnover velocity. Due to the rapid de-correlation between the horizontal velocity and temperature, the covariance $\overline{u'T'}$ rapidly decays under unstable conditions[13] while $\overline{T'T'}$ becomes larger compared to its neutral value. Consequently, it is clear that

a major modification to the earlier phenomenological model must include, at minimum, the effect of the temperature variance on heat transfer. It can be also argued that within the inertial subrange (as we assumed here), $\overline{u'T'}$ decays as $k^{-7/3}$ while $\overline{T'T'}$ decays as $k^{-5/3}$, clearly indicating that the role of buoyancy is more important for heat than for momentum.[21]

With regards to framing this modification via an effective adjustment to the attached eddy size ($= z$), note that upon combining $\sigma_T^2/T_*^2 = \varphi_{TT}(\varsigma)$, the Monin-Obukhov variance-flux similarity relation with $T_* = \dfrac{d\overline{T}}{dz}\dfrac{\kappa_v z}{\phi_h(\varsigma)}$ results in $\sigma_T = \left(\dfrac{d\overline{T}}{dz}\right) z\left(\kappa_v \dfrac{\sqrt{\varphi_{TT}(\varsigma)}}{\phi_h(\varsigma)}\right)$. Substituting this expression into Eq. (A8) gives

$$\begin{aligned}\overline{w'T'} &= \frac{\tau}{C_2}\left(-\sigma_w^2\frac{d\overline{T}}{dz} + \frac{4}{3}\frac{g}{\overline{T}}\sigma_T\frac{d\overline{T}}{dz}z\left(\kappa_v\frac{\sqrt{\varphi_{TT}(\varsigma)}}{\phi_h(\varsigma)}\right)\right)\\ &= -\sigma_w\frac{d\overline{T}}{dz}\frac{\sigma_w\tau}{C_2}\left(1+\frac{\frac{4}{3}\frac{g}{\overline{T}}\sigma_T z\left(\kappa_v\frac{\sqrt{\varphi_{TT}(\varsigma)}}{\phi_h(\varsigma)}\right)}{-\sigma_w\frac{\sigma_w\tau}{C_2}}\right)\\ &\sim -v(s)\frac{d\overline{T}}{dz}sf_T(\varsigma).\end{aligned} \tag{A9}$$

In Eq. (A9), $f_T(\varsigma)$ can be seen as a "correction" of the length scale (s) due to the effect of the temperature variance. This is consistent with our analyses that the potential scale-resonance between the turnover eddy and the excursions in the temperature profile (Fig. 5) requires a new length scale introduced to the model when extending it to temperature, as shown in Eq. (14).

APPENDIX B: A NEW THEORETICAL DERIVATION FOR AN O'KEYPS EQUATION FOR TEMPERATURE

In this appendix, it is demonstrated that an O'KEYPS equation describing the heat stability correction function can be derived from inertial subrange scaling provided the mean temperature difference across a turnover eddy linearly scales with the macro-scale properties of the eddy. This derivation commences with the phenomenological model for sensible heat flux, $\overline{w'T'} = -\alpha_h v(s)\left[\overline{T}(z+s) - \overline{T}(z-s)\right]$ and $v(s) = \overline{\Delta w(s)^2}^{1/2}$. Postulating that the mean temperature difference across a turnover eddy is now entirely described by the macro-scale properties of the eddy, which are due to the large and often coherent ramp-like structures simultaneously contributing to the mean temperature gradient and macro-scale temperature difference, implies that $\left[\overline{T}(z+s) - \overline{T}(z-s)\right] \sim \overline{(T'(z+s) - T'(z-s))^2}^{1/2} \sim \overline{(\Delta T(s))^2}^{1/2}$. For notational simplicity, denote $|\Delta\psi(s)| = (\psi'(x+s) - \psi'(x-s))^2$ for any arbitrary flow variable ψ.

From the Kolmogorov theory for the velocity spectrum and the Kolmogorov-Corrsin theory for the temperature spectrum,[32] $|\Delta w(s)| = C_o\varepsilon^{1/3}s^{1/3}$, and $|\Delta T(s)| = C_T\chi_T^{1/2}\varepsilon^{-1/6}s^{1/3}$, where C_o and C_T are related to the Kolmogorov constant. Here, χ_T is the dissipation rate for the temperature variance. Hence, at $s = z$ and with $\overline{w'T'} = -T_*u_*$, the sensible heat flux is now given as

$$\frac{\alpha_h C_T C_o \chi_T^{1/2}\varepsilon^{1/6}z^{2/3}}{T_*u_*} = 1. \tag{B1}$$

As per Eq. (7), $\varepsilon = \frac{u_*^3}{\kappa_v z}(\phi_m(\varsigma) - \varsigma)$, and by invoking the local equilibrium assumption stating that the dissipation rate is equal to the production rate for the mean temperature variance,[33] namely, $\chi_T = -\overline{w'T'}\dfrac{d\overline{T}}{dz} = u_*\dfrac{T_*^2}{\kappa_v z}\phi_h(\varsigma)$, we obtain

$$\frac{\alpha_h C_T C_o\left(u_*\frac{T_*^2}{\kappa_v z}\phi_h(\varsigma)\right)^{1/2}\left(\frac{u_*^3}{\kappa_v z}(\phi_m(\varsigma) - \varsigma)\right)^{1/6}z^{2/3}}{T_*u_*} = 1. \tag{B2}$$

Simplifying this expression further leads to

$$\left(\frac{\alpha_h C_T C_o}{\kappa_v^{2/3}}\right)\phi_h(\varsigma)^{1/2}\left(\phi_m(\varsigma)-\varsigma\right)^{1/6}=1. \tag{B3}$$

Again, upon imposing $\phi_h(0)=\phi_m(0)=1$ for $\varsigma=0$, Eq. (B3) yields

$$\left[\phi_h(\varsigma)\right]^3\phi_m(\varsigma)\left(1-\frac{\varsigma}{\phi_m(\varsigma)}\right)=1. \tag{B4}$$

It is evident that this formula is identical to Eq. (9), which was a straightforward extension of the original phenomenological model. When $\phi_h(\varsigma)=\phi_m(\varsigma)$, it also recovers the canonical form of the O'KEYPS equation,[12] or Eq. (8).

Furthermore, deviations from the canonical energy cascade and temperature variance cascade can be readily accounted for via intermittency corrections $(s/I_w)^{\mu_1}$ and $(s/I_T)^{\mu_2}$, respectively, where I_w and I_T are the integral length scales for vertical velocity and temperature, and μ_1 and μ_2 are the intermittency correction coefficients.[34,35]

These intermittency corrections result in $|\Delta w(s)|=C_o\varepsilon^{1/3}s^{1/3}(s/I_w)^{\mu_1}$ and $|\Delta T(s)|=C_T\chi_T^{1/2}\varepsilon^{-1/6}s^{1/3}(s/I_T)^{\mu_2}$. Similar to previous derivations, the final outcome with these intermittency corrections is

$$\left[\phi_h(\varsigma)\right]^3\phi_m(\varsigma)\left(1-\frac{\varsigma}{\phi_m(\varsigma)}\right)=\frac{1}{g_w^{6\mu_1}g_T^{6\mu_2}}, \tag{B5}$$

where $g_w=\dfrac{z}{I_w}$ and $g_T=\dfrac{z}{I_T}$. Note that g_w and g_T vary with the integral length scales I_w and I_T, as previously demonstrated in Eq. (16). In addition, as discussed in Warhaft,[24] ramp-cliff structures in the temperature field result in $\mu_1\le\mu_2$,which appears to be qualitatively consistent with Eq. (16) given that the differences here between ϕ_h and ϕ_m also originate from variations in the temperature gradient scale caused by ramps (i.e., large-scale impacting inertial subrange) on intermittency parameters.

[1] W. Brutsaert, *Hydrology: An Introduction* (Cambridge University Press, New York, 2005).
[2] A. S. Monin and A. M. Obukhov, "Basic laws of turbulent mixing in the ground layer of the atmosphere," Akad. Nauk. SSSR, Geofiz. Inst. Trudy **151**, 163 (1954).
[3] R. B. Stull, *An Introduction to Boundary Layer Meteorology* (Kluwer Academic, Dordrecht, 1988).
[4] W. Brutsaert, *Evaporation into the Atmosphere: Theory, History, and Applications* (Reidel, Dordrecht, 1982), Environmental fluid mechanics.
[5] J. A. Businger, "A note on the Businger-Dyer profiles," Boundary-Layer Meteorol. **42**, 145 (1988).
[6] J. Vilà-Guerau de Arellano, P. G. Duynkerke, and K. F. Zeller, "Atmospheric surface-layer similarity theory applied to chemically reactive species," J. Geophys. Res., [Atmos.] **100**, 1397, doi:10.1029/94JD02434 (1995).
[7] S. Khanna and J. G. Brasseur, "Analysis of Monin-Obukhov similarity from large-eddy simulation," J. Fluid Mech. **345**, 251 (1997).
[8] U. Hogstrom, "Non-dimensional wind and temperature profiles in the atmospheric surface-layer - A re-evaluation," Boundary-Layer Meteorol. **42**, 55 (1988).
[9] D. K. Wilson, "An alternative function for the wind and temperature gradients in unstable surface layers - Research note," Boundary-Layer Meteorol. **99**, 151 (2001).
[10] B. A. Kader and A. M. Yaglom, "Mean fields and fluctuation moments in unstably stratified turbulent boundary-layers," J. Fluid Mech. **212**, 637 (1990).
[11] G. Gioia *et al.*, "Spectral theory of the turbulent mean-velocity profile," Phys. Rev. Lett. **105**, 184501 (2010).
[12] G. G. Katul, A. G. Konings, and A. Porporato, "Mean velocity profile in a sheared and thermally stratified atmospheric boundary layer," Phys. Rev. Lett. **107**, 268502 (2011).
[13] D. Li and E. Bou-Zeid, "Coherent structures and the dissimilarity of turbulent transport of momentum and scalars in the unstable atmospheric surface layer," Boundary-Layer Meteorol. **140**, 243 (2011).
[14] E. Bou-Zeid *et al.*, "Field study of the dynamics and modelling of subgrid-scale turbulence in a stable atmospheric surface layer over a glacier," J. Fluid Mech. **665**, 480 (2010).
[15] A. A. Townsend, *The Structure of Turbulent Shear Flow*, 2nd ed. (Cambridge University Press, Cambridge, England, 1976), Cambridge monographs on mechanics and applied mathematics.
[16] A. J. Smits, B. J. McKeon, and I. Marusic, "High-Reynolds number wall turbulence," Annu. Rev. Fluid Mech. **43**, 353 (2011).
[17] J. A. Businger and A. M. Yaglom, "Introduction to Obukhov's paper on 'turbulence in an atmosphere with a non-uniform temperature'," Boundary-Layer Meteorol. **2**, 3 (1971).
[18] N. Vercauteren *et al.*, "Subgrid-scale dynamics of water vapour, heat, and momentum over a lake," Boundary-Layer Meteorol. **128**, 205 (2008).

[19] E. Bou-Zeid *et al.*, "Scale dependence of subgrid-scale model coefficients: An *a priori* study," Phys. Fluids **20**, 115106 (2008).
[20] D. Li, E. Bou-Zeid, and H. De Bruin, "Monin–Obukhov similarity functions for the structure parameters of temperature and humidity," Boundary-Layer Meteorol. **145**(1), 45–67 (2012).
[21] J. C. Kaimal and J. J. Finnigan, *Atmospheric Boundary Layer Flows: Their Structure and Measurement* (Oxford University Press, New York, 1994).
[22] A. Kolmogoroff, "The local structure of turbulence in incompressible viscous fluid for very large Reynolds numbers," C. R. Acad. Sci. URSS **30**, 301 (1941).
[23] S. Corrsin, "On the spectrum of isotropic temperature fluctuations in an isotropic turbulence," J. Appl. Phys. **22**, 469 (1951).
[24] Z. Warhaft, "Passive scalars in turbulent flows," Annu. Rev. Fluid Mech. **32**, 203 (2000).
[25] W. M. Kays, "Turbulent Prandtl number - Where are we," J. Heat Transfer **116**, 284 (1994).
[26] M. Siqueira and G. Katul, "Estimating heat sources and fluxes in thermally stratified canopy flows using higher-order closure models," Boundary-Layer Meteorol. **103**, 125 (2002).
[27] T. Meyers and K. T. P. U, "Testing of a higher-order closure-model for modeling air-flow within and above plant canopies," Boundary-Layer Meteorol. **37**, 297 (1986).
[28] C. H. Moeng and J. C. Wyngaard, "An analysis of closures for pressure-scalar covariances in the convective boundary-layer," J. Atmos. Sci. **43**, 2499 (1986).
[29] S. E. Belcher and J. C. R. Hunt, "Turbulent flow over hills and waves," Annu. Rev. Fluid Mech. **30**, 507 (1998).
[30] G. G. Katul, A. M. Sempreviva, and D. Cava, "The temperature-humidity covariance in the marine surface layer: A one-dimensional analytical model," Boundary-Layer Meteorol. **126**, 263 (2008).
[31] D. Cava *et al.*, "Buoyancy and the sensible heat flux budget within dense canopies," Boundary-Layer Meteorol. **118**, 217 (2006).
[32] A. S. Monin and A. M. Yaglom, *Statistical Fluid Mechanics* (MIT, Cambridge, MA, 1975).
[33] C. I. Hsieh and G. G. Katul, "Dissipation methods, Taylor's hypothesis, and stability correction functions in the atmospheric surface layer," J. Geophys. Res., [Atmos.] **102**, 16391, doi:10.1029/97JD00200 (1997).
[34] A. N. Kolmogorov, "A refinement of previous hypotheses concerning the local structure of turbulence in a viscous incompressible fluid at high Reynolds number," J. Fluid Mech. **13**, 82 (1962).
[35] U. Frisch, *Turbulence: The Legacy of A.N. Kolmogorov* (Cambridge University Press, Cambridge, England, 1995).